Original Article

Biomechanical and Histomorphometric Characterizations of Osseointegration during Mini-Screw Healing in Rabbit Tibiae*

Jing Wu[a]; Yu-Xing Bai[b]; Bang-Kang Wang[b]

ABSTRACT

Objective: To evaluate effects of different healing times on integration of titanium mini-screws and bones under unloaded conditions.

Materials and Methods: Biomechanical stability measurements and histomorphometric observations were performed in a rabbit tibia model after different healing times: 0 (immediate) and 1, 2, 4, and 8 weeks.

Results: Biomechanical stability and both maximum torque and maximum pullout load increased with healing time but increased significantly only after 4 weeks. Maximum torque and maximum pullout load both significantly correlated with healing time and with each other. Similarly, histomorphometric analyses showed that new bone formation increased with healing time but increased dramatically only after 4 weeks. The data may provide guidance for determining optimal implant plans in clinical practice.

Conclusion: Mini-screw healing is a continuous process, and week 4 is a critical time point in this process. (*Angle Orthod.* 2009;79:558–563.)

KEY WORDS: Implant anchorage; Mini-screw; Healing; Biomechanical testing; Histomorphometry

INTRODUCTION

Good anchorage control is one of the prerequisites to successful orthodontic therapy. It affects not only treatment plans but also results. Recently, mini-implant anchors, particularly titanium mini-screws, have attracted orthodontists' attention for their advantages: flexibility in choosing implant locations, lower medical costs, simpler implant surgery, and lower degrees of discomfort after implantation compared with traditional dental implants.[1–4] However, these mini-screws loosen easily or even break and their stability must be further investigated.[1–4] Increasing knowledge about the healing phase is important for an understanding of factors that are required to achieve implant-bone integration and to identify the optimal time of initial loading. Too little or too late loading may result in reduced stability at implant-bone interfaces and bone atrophy. On the other hand, too much or too early loading may loosen implant-bone interfaces and cause bone damage.[5,6] Initial loading time varies a lot in clinical case reports and animal studies.[7–11] In this study, a rabbit tibia model was used to examine the effects of different healing times on biomechanical stability and histomorphometric characteristics during integration of mini-screws and bones.

MATERIALS AND METHODS

Animals

A total of 15 male, 3-month-old New Zealand White rabbits (mean weight, 4.0 kg) were randomly divided into five groups with different healing times: 0 (immediate) and 1, 2, 4, and 8 weeks. Ten animals were subjected to mechanical tests and the other five to histomorphometric studies. All animal protocols were approved by The Beijing Hospital of Stomatology and Capital University of Medical Sciences (SYXK2005-0031) (Beijing, China).

[a] Assistant Professor, Department of Orthodontics, Capital Medical University, School of Stomatology, Beijing, China.

[b] Professor, Department of Orthodontics, Capital Medical University, School of Stomatology, Beijing, China.

Corresponding author: Dr Jing Wu, Department of Orthodontics, Capital Medical University, School of Stomatology, #4 Tian tan xi li, Chongwen district, Beijing, Beijing 100050 China (e-mail: crystalwupaper@gmail.com)

Accepted: July 2008. Submitted: March 2008.

*This work was supported by the Capital Medical Development and Research Fund, Beijing Medicine and Technology Key Project (2005-2017).

Implants

Ninety titanium mini-screws, 6.0 mm long and 1.9 mm in diameter, were used in this study. All implants were custom-made of c.p. titanium (Medicon, Tuttlingen, Germany). Before experiments were performed, all implants were cleaned ultrasonically in butanol and absolute ethanol for 10 minutes. Sixty implants were used for mechanical tests, and the other 30 for histomorphometric studies.

Surgical Procedures

All surgeries were performed under sterile conditions in an animal operation room. The animals were anesthetized with an intramuscular injection of ketamine (10 mg/kg). The local nerve supplies of the internal surface of the tibia were further blocked with 0.5 mL of 2% lidocaine. Both tibial metaphyses were chosen as experimental sites and were exposed through curved skin incisions. The mid-diaphyseal surface of the tibia was surgically exposed by blunt dissection. A guide drill was used first to mark the implant sites approximately 10 mm apart, with three implants on each tibia. Room temperature saline was used to prevent overheating of the drilling sites. Implants were inserted into cortical layers manually with care. The surgical wounds were closed in layers. All animals were given antibiotics for 3 days after surgery.

Mechanical Tests

After 0, 1, 2, 4, or 8 weeks of healing, in vivo mechanical tests were performed. The animals were anesthetized as described above. Surgical areas were carefully dissected to avoid any preload application to the mini-screws. (1) Removal torque test. An electronic torque meter (model WD-4020, specially designed by Digital Torque Measurement Co, Beijing, China) was used to assess the maximum torque (Ncm) required to loosen the implants. (2) Pullout test. A multifunction electronic meter (model M10~M200, Minfeng Trading Co Ltd, Shanghai, China) was used to measure the maximum load (N) required to pull out the implants. All animals were euthanized when the experiments had been completed.

Histomorphometric Analyses

The animals were sacrificed by an intravenous overdose of pentobarbital. The implants, together with surrounding bone and soft tissues, were removed and were fixed in 10% buffered formaldehyde for the following histomorphometric analyses. (1) Polarized light microscopic analysis and toluidine blue staining (nondecalcified). After embedding in polyacrylate, samples were cut and ground to about 60-μm-thick serial sections, parallel to the long axis of the mini-screws. Sections first were examined with polarized light microscope and then were stained with toluidine blue for further analysis. (2) Hematoxylin and eosin staining (decalcified). Samples were fixed in 10% buffered formaldehyde solution (pH 7.4) at 4°C for 1day and were decalcified in a mixture of formic acid and sodium citrate at 4°C for 6 days. The samples were embedded in paraffin, cut into ~7- to ~8-μm serial sections, and stained with hematoxylin and eosin (H&E). (3) Scanning electron microscopic analysis. The implant-bone units were cut longitudinally and were fixed for histomorphometric examination with the scanning electron microscope.

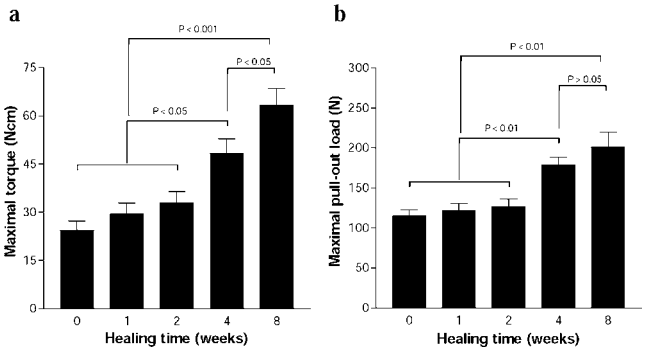

Figure 1. Biomechanical measurements after different healing times. (a) Maximum torque at different time points. (b) Maximum pullout load at different time points. Statistical analyses are shown on the graphs.

Statistical Analyses

Differences between groups were analyzed with Student's *t*-test. Correlations between groups were analyzed with the nonparametric permutation test.

RESULTS

Time-Dependent Increase in Maximum Torque and Maximum Pullout Load

The maximum torque and pullout load reflect the degree of integration of titanium mini-screws and bones.[12] Removal torque tests measure the biomechanics on the implant-bone interfaces, and pullout tests probe the biomechanical properties of the bones surrounding the implants.[12]

Our results showed that the longer the healing time, the larger was the torque or pullout load required to remove the implants (Figure 1a,b). However, only after 4 weeks of healing did the maximum torque and maximum pullout load increase significantly (Figure 1a,b), indicating that 4 weeks is an important time point for implant-bone units to gain biomechanical strength and integration. The maximum torque further increased

Table 1. Correlation Between Healing Time, Maximal Torque, and Maximal Pullout Load[a]

	Healing Time	Maximal Torque	Maximal Pullout Load
Healing time	—	$r = .788$ $P < .0001$	$R = .811$ $P < .0001$
Maximal torque	$r = .788$ $P < .0001$		$R = .601$ $P < .001$

[a] *r* indicates Pearson correlation coefficient.

significantly after 8 weeks of healing (Figure 1a), but the maximum pullout load did not (Figure 1b).

Positive Correlations Between Healing Time, Maximum Torque, and Maximum Pullout Load

The relationships between healing time, maximum torque, and maximum pullout load were further analyzed by the nonparametric permutation test. Both maximum torque and maximum pullout load significantly correlated with healing time (Table 1). Maximum torque and maximum pullout load correlated with each other significantly as well (Table 1). All correlations were positive, suggesting that implant-bone units gained their biomechanical strength over time.

Histomorphometric Analyses Showing Time-Dependent New Bone Growth

Specimens obtained immediately after mini-screw insertion (0 week) and after 1, 2, 4, or 8 weeks of healing were analyzed under light microscope and scanning electron microscope. Immediately (0 week) after mini-screw insertion, implant-bone interfaces were filled with erythrocytes and debris under polarized light microscopic analysis and toluidine blue staining (Figure 2a,b). After decalcification and H&E staining, implant-bone interfaces appeared to be smooth (Figure 2c). These observations revealed no new bone formation at this stage.

After 1 week of healing, collagen fibers and granulation tissues were found on implant-bone interfaces under polarized light microscopic analysis and toluidine blue staining (Figure 3a,c). In areas close to endostea, tiny trabeculae were growing toward the implants (Figure 3b,d). After decalcification and H&E staining, implant-bone interfaces still appeared to be smooth (Figure 3e). Inflammatory cells, mainly macrophages, were observed on the implant-bone interfaces under scanning electron microscopic analysis (Figure 3f). These macrophages showed extensive spreading, large surface areas, and prominent ruffled membranes and filopodia. These histomorphometric characters revealed a stage of inflammatory response and the beginning of new bone growth.

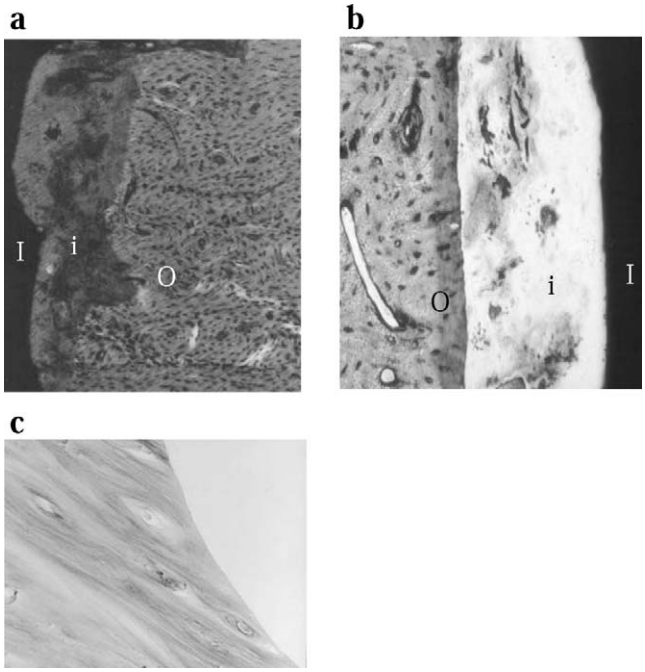

Figure 2. Histomorphometric analyses immediately after mini-screw insertion. (a) Polarized light microscopic image (10×). I indicates implant; i, interface; and O, old bone. (b) Toluidine blue staining (20×). The implant-bone interface is filled with erythrocytes and debris. (c) Hematoxylin and eosin (H&E) staining (20×). I indicates the location of the implant that disassociated from bone tissue during the processing procedure of decalcification. The erythrocytes and debris on the implant-bone interface also are dislocated.

After 2 weeks of healing, implant-bone interfaces were surrounded by large amounts of fibers and connective tissue under polarized light microscopic analysis and toluidine blue staining (Figure 4a,c). In areas close to endostea were small trabeculae, primarily a lattice of bones with random structures, growing toward the implants (Figure 4b,d). H&E staining showed thin layers of collage fiber bundles formed on implant-bone interfaces, dense on the implant side and loose on the old bone side (Figure 4e). Osteoblasts, fibroblasts, and collagen fibers were observed under scanning electron microscopic analysis (Figure 4f,g). Osteoblasts are polygonal or oval, and fibroblasts are star-like, spindle-like, or irregular. These histomorphometric characteristics revealed a stage of increasing new bone growth.

After 4 weeks of healing, new bone, particularly woven bone (W), was observed on implant-bone interfaces (Figure 5a,c) and endosteal surfaces under polarized light microscopic analysis and toluidine blue staining (Figure 5b,d). H&E staining also showed apparent new bone formation with large trabeculae on the implant-bone interfaces (Figure 5e) and a noncalcified matrix between the trabeculae (Figure 5f). The new bones have a distinct growth direction (almost

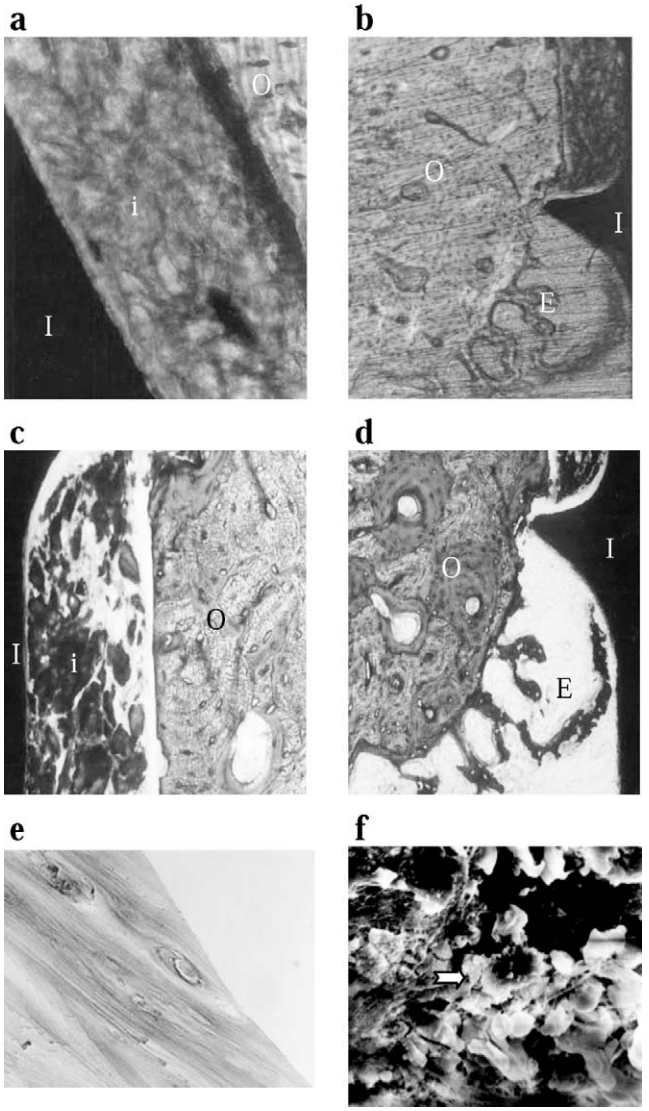

Figure 3. Histomorphometric analyses 1 week after mini-screw insertion. (a) Polarized light microscopic image shows collagen fibers and granulation tissues on the implant-bone interface (40×). I indicates implant; i, interface; and O, old bone. (b) Polarized light microscopic image shows tiny trabeculae growing toward the implant (10×). E indicates endostea. (c) Toluidine blue staining shows collagen fibers and granulation tissues on the implant-bone interface (20×). (d) Toluidine blue staining shows tiny trabeculae growing toward the implant (10×). (e) H&E staining (20×). I indicates the location of the implant that disassociated from bone tissue during the processing procedure of decalcification. (f) Scanning electron microscopic image (1500×). A macrophage is illustrated by the arrow.

perpendicular) compared with the old bones, and clear edges can be seen between new and old bones (Figure 5e,f). Scanning electron microscopic analysis revealed that at this stage, osteoblasts were clustering together (Figure 5g) and were forming woven trabeculae (Figure 5h). Needle- or flake-shaped woven trabeculae connect to each other to form grid structures. These histomorphometric characteristics revealed a dynamic bone growth stage.

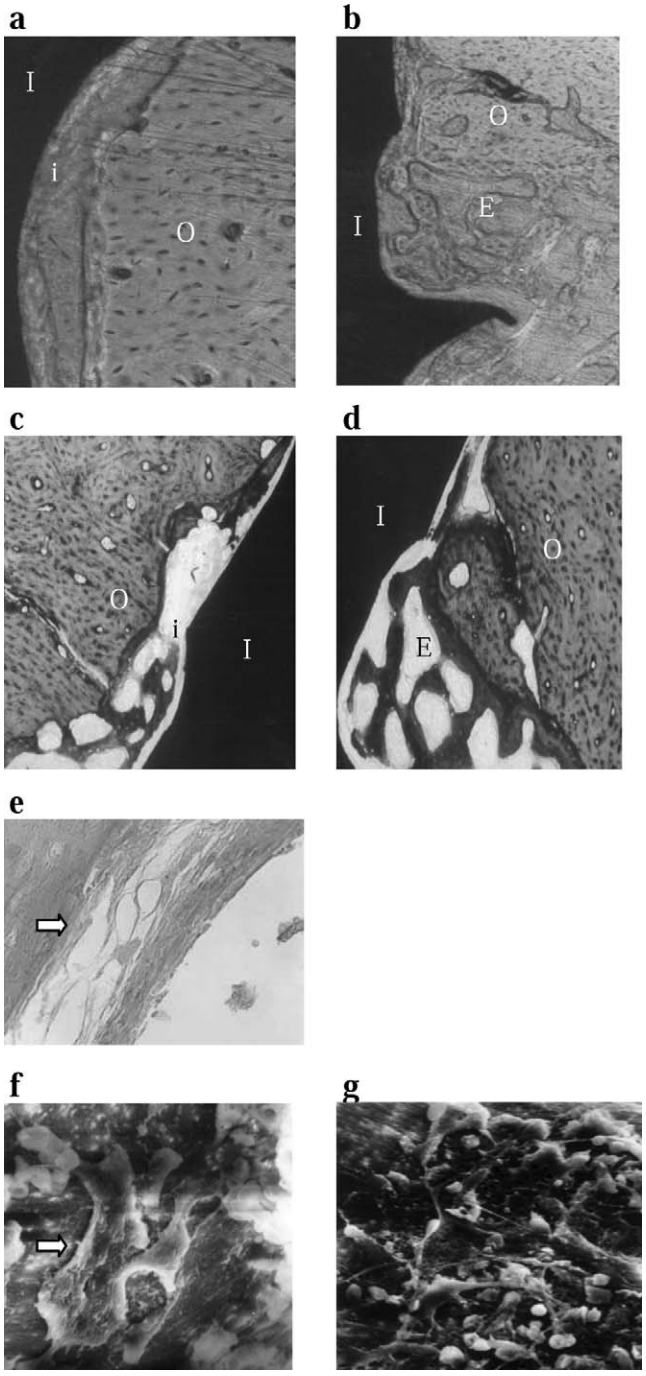

Figure 4. Histomorphometric analyses 2 weeks after mini-screw insertion. (a) Polarized light microscopic image shows fibers and connective tissue on the implant-bone interface (10×). I indicates implant; i, interface; and O, old bone. (b) Polarized light microscopic image shows small trabeculae growing toward the implant (10×). E indicates endostea. (c) Toluidine blue staining shows fibers and connective tissue on the implant-bone interface (10×). (d) Toluidine blue staining shows small trabeculae growing toward the implant (10×). (e) H&E staining (20×). I indicates the location of the implant that disassociated from bone tissue during the processing procedure of decalcification. Collagen fiber bundles are illustrated by the arrow. (f) Scanning electron microscopic image (1200×). An osteoblast is illustrated by the arrow. (g) Scanning electron microscopic image (1000×). The area is filled with osteoblasts, fibroblasts, and collagen fibers.

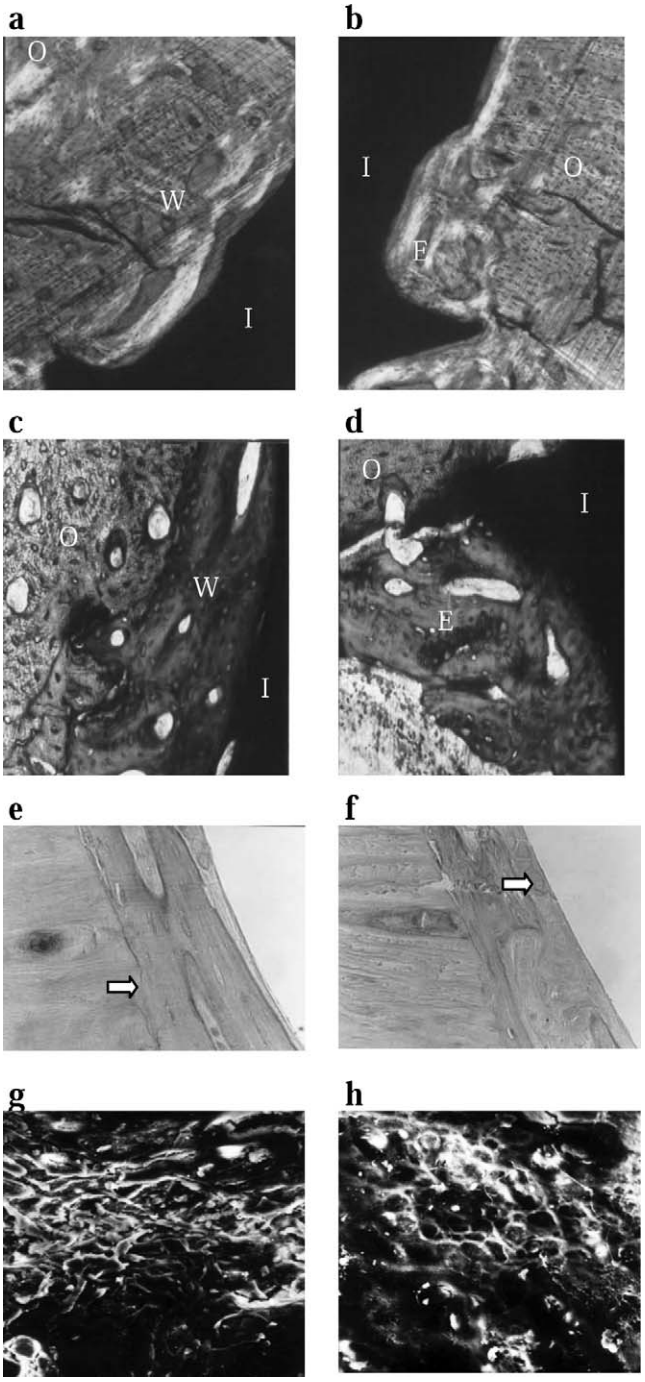

Figure 5. Histomorphometric analyses 4 weeks after mini-screw insertion. (a) Polarized light microscopic image shows woven bones on the implant-bone interface (10×). I indicates implant; W, woven bone; and O, old bone. (b) Polarized light microscopic image shows woven bones near the endosteal surface (10×). E indicates endostea. (c) Toluidine blue staining shows woven bones on the implant-bone interface (20×). (d) Toluidine blue staining shows woven bones near the endosteal surface (20×). (e) H&E staining shows a large trabecula (illustrated by the arrow) (20×). I indicates the location of the implant that disassociated from bone tissue during the processing procedure of decalcification. (f) H&E staining shows noncalcified matrix (illustrated by the arrow) (20×). (g) Scanning electron microscopic image shows clustered osteoblasts (400×). (h) Scanning electron microscopic image shows woven trabeculae (700×).

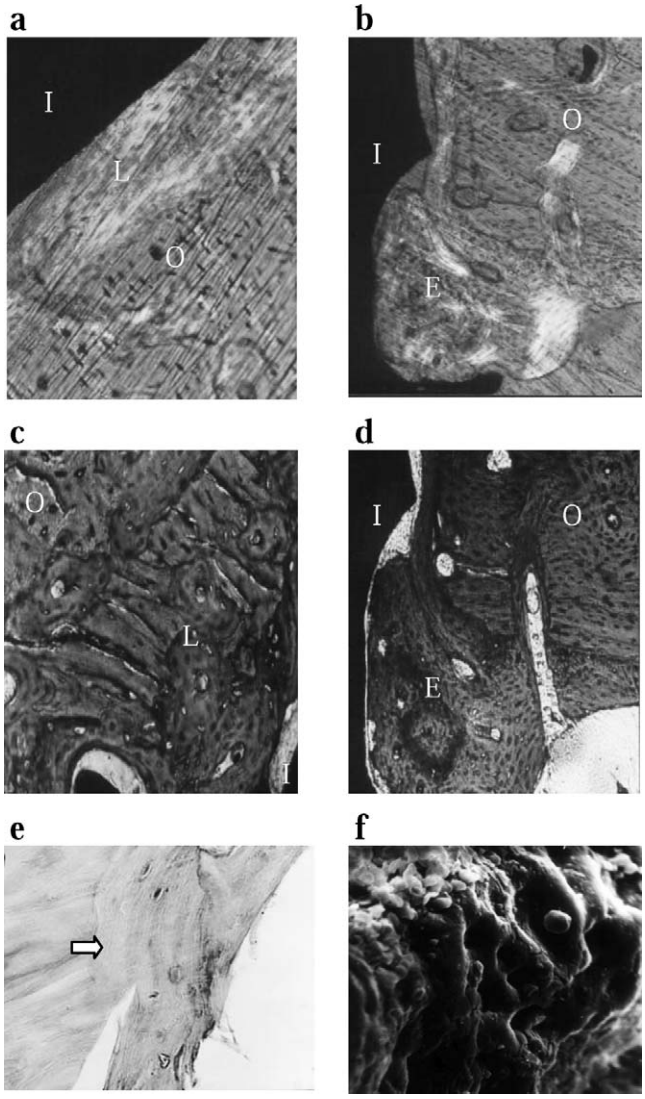

Figure 6. Histomorphometric analyses 8 weeks after mini-screw insertion. (a) Polarized light microscopic image shows lamellae formation on the implant-bone interface (20×). I indicates implant; L, lamellae; and O, old bone. (b) Polarized light microscopic image shows mature and highly calcified bones near the endostea (10×). E indicates endostea. (c) Toluidine blue staining shows lamellae formation on the implant-bone interface (10×). (d) Toluidine blue staining shows mature and highly calcified bones near the endostea (10×). (e) H&E staining shows lamellar remodeling (illustrated by the arrow) (20×). I indicates the location of the implant that disassociated from bone tissue during the processing procedure of decalcification. (f) Scanning electron microscopic image shows mature lacunae (1000×).

After 8 weeks of healing, mature, compact, and highly calcified bones such as lamellae (L) were observed under polarized light microscopic analysis and toluidine blue staining (Figure 6a,c). Bones near endostea also were mature and highly calcified (Figure 6b,d). H&E staining revealed that many lamellae were compact and had similar degree of calcification compared with the old bones, and that the edges between

the new and old bones became blurred by lamellar remodeling (Figure 6e). Osteoblasts were found in mature lacunae during scanning electron microscopic analysis (Figure 6f). These histomorphometric characteristics suggested a mature bone growth stage.

DISCUSSION

Branemark et al[12] studied mini-implants using rat tibia, but the method that was used to assess biomechanical and histologic characteristics was not ideal because the same fixture was used for torque test, then pullout test, and finally histomorphometric examination. Here we used rabbit tibia to study biomechanical and histomorphometric changes during the integration process of mini-screws in parallel cohorts for the purpose of obtaining a more accurate assessment of these important issues.

Maximum torque and maximum pullout load were used to characterize biomechanical strength. Both parameters increased with healing time (Figure 1). Four weeks is a critical time point at which biomechanical strength was first observed to increase significantly (Figure 1). These results are comparable with those obtained in rat tibiae.[12] Histomorphometric results obtained with polarized light microscopic analysis and toluidine blue staining, H&E staining, and scanning electron microscopic analysis further support that 4 weeks is a crucial time point, at which abundant new bone formation was observed (Figure 5), although occasionally, new bones were noticed as early as the 1-week time point (Figure 3).

Optimal loading time is critical to successful therapy in orthodontics.[11] The results of this study show that during the first 2 weeks, integration of titanium mini-screws and bones was weak (Figures 1 and 4), and loading during this time may not be appropriate. After 4 weeks of healing, integration of titanium mini-screws and bones was significantly stronger (Figures 1 and 5), and loading at this time point should be safe. Four weeks is a critical time point during the progress of integration of titanium mini-screws and bones. After 8 weeks of healing, both biomechanical stability and histomorphometric implant-bone interfaces continued to increase (Figures 1 and 6), suggesting that larger loading is safe between ~4 and ~8 weeks. These data may serve as the basis for additional clinical studies in humans to help orthodontists choose optimal implant plans and achieve more successful treatment outcomes.

CONCLUSION

- Loading during the first 2 weeks of healing time would damage the stability of the implant-bone fixture. Therefore, we do not recommend loading during this period.
- After 4 weeks, the implant-bone fixture is strong enough to support loading. Loading at this time is recommended.
- After 8 weeks, loading is still safe. Therefore, at least a 4-week window is suitable for loading.

REFERENCES

1. Miyawaki S, Koyama I, Inoue M, Mishima K, Sugahara T, Takano-Yamamoto T. Factors associated with the stability of titanium screws placed in the posterior region for orthodontic anchorage. *Am J Orthod Dentofacial Orthop.* 2003; 124:373–378.
2. Simon H, Caputo AA. Removal torque of immediately loaded transitional endosseous implants in human subjects. *Int J Oral Maxillofac Implants.* 2002;17:839–845.
3. Bae SM, Park HS, Kyung HM, Kwon OW, Sung JH. Clinical application of micro-implant anchorage. *J Clin Orthod.* 2002; 36:298–302.
4. Lee JS, Park HS, Kyung HM. Micro-implant anchorage for lingual treatment of a skeletal Class II malocclusion. *J Clin Orthod.* 2001;35:643–647. quiz 620.
5. Frost HM. Wolff's law and bone's structural adaptations to mechanical usage: an overview for clinicians. *Angle Orthod.* 1994;64:175–188.
6. Meijer HJ, Steen WH, Bosman F. A comparison of methods to assess marginal bone height around endosseous implants. *J Clin Periodontol.* 1993;20:250–253.
7. Cheng SJ, Tseng IY, Lee JJ, Kok SH. A prospective study of the risk factors associated with failure of mini-implants used for orthodontic anchorage. *Int J Oral Maxillofac Implants.* 2004;19:100–106.
8. Deguchi T, Takano-Yamamoto T, Kanomi R, Hartsfield JK Jr, Roberts WE, Garetto LP. The use of small titanium screws for orthodontic anchorage. *J Dent Res.* 2003;82: 377–381.
9. Melsen B, Lang NP. Biological reactions of alveolar bone to orthodontic loading of oral implants. *Clin Oral Implants Res.* 2001;12:144–152.
10. Ohmae M, Saito S, Morohashi T, Seki K, Qu H, Kanomi R, et al. A clinical and histological evaluation of titanium mini-implants as anchors for orthodontic intrusion in the beagle dog. *Am J Orthod Dentofacial Orthop.* 2001;119:489–497.
11. Roberts WE, Smith RK, Zilberman Y, Mozsary PG, Smith RS. Osseous adaptation to continuous loading of rigid endosseous implants. *Am J Orthod.* 1984;86:95–111.
12. Branemark R, Ohrnell LO, Nilsson P, Thomsen P. Biomechanical characterization of osseointegration during healing: an experimental in vivo study in the rat. *Biomaterials.* 1997; 18:969–978.